$N\Sigma_c$ and $N\Sigma_b$ resonances in the quark-delocalization color-screening model

Hongxia Huang,[1] Jialun Ping,[1] and Fan Wang[2]

[1]*Department of Physics, Nanjing Normal University, Nanjing 210097, People's Republic of China*
[2]*Department of Physics, Nanjing University, Nanjing 210093, People's Republic of China*

The $N\Lambda_c$ and $N\Lambda_b$ systems with $I = \frac{1}{2}$ and $J^P = 0^+$ or 1^+ are investigated within the framework of the quark delocalization color screening model (QDCSM) by solving a resonating group method equation. The results show that the interaction between N and Λ_c is attractive, but it is not strong enough to form any $N\Lambda_c$ bound state, even with the help of channel coupling. Whereas the attraction between N and Σ_c is strong enough to form a bound state $N\Sigma_c(^3S_1)$, it becomes a resonance state with the resonance mass of 3389–3404 MeV by coupling to the open $N\Lambda_c$ D-wave channel. However it does not show up in the $N\Lambda_c$ S-wave channel. The corresponding states $N\Lambda_b$, $N\Sigma_b$ have similar properties as that of states $N\Lambda_c$, $N\Sigma_c$, and there exists a $N\Sigma_b(^3S_1)$ resonance state with energy of 6733–6743 MeV in the $N\Lambda_b$ D-wave scattering phase shifts.

I. INTRODUCTION

Understanding the hadron-hadron interactions and exotic quark states is one of the important topics in temporary hadron physics. On the hadron level, various sophisticated coupled-channel approaches have been formulated to study this topic. On the quark level, several constituent quark models have also been developed to investigate hadron-hadron interactions. Generally these two approaches give coincident results. For example, the quantitative descriptions of nucleon-nucleon (NN), hyperon-nucleon (YN), and hyperon-hyperon interactions have been achieved in the hadron level approaches, one-boson-exchange (OBE) models [1,2], the chiral perturbation theory [3], and in the quark level approaches, chiral quark model [4–6], quark delocalization color screening model [7–9], and so on. Recently, the study of the hadron-hadron interaction is extended to the heavy hadron systems. The $\Sigma_c\bar{D}$-$\Lambda_c\bar{D}$ system was studied in the coupled-channel unitary approach with the local hidden gauge formalism and the chiral constituent quark models. A $\Sigma_c\bar{D}$ bound state with energy around 4.3 GeV was obtained in these two approaches [10,11], again a coincident result is obtained. However, the models on the hadron level and on the quark level do not always give the same results. For example, on the hadron level, the Roper resonance can be described by meson-baryon dynamics alone and no genuine $N^*(1440)$ resonance is needed in a coupled-channel meson exchange model [13]. While on the quark level, the baryon resonances are described as the excited states of three constituent quarks [14]. In the chiral quark model, some nucleon resonances can be accommodated as baryon-meson dynamically generated resonances [15]. Thus, different models may give different descriptions for the resonance structures.

Since the prediction of charmed hypernuclei in the mid-1970s [16,17], extensive studies of hypernuclei with heavy flavors have been carried out [18–20]. The observation of Λ_c nuclei had been claimed [21]. The experimental search of the charmed and bottom hypernuclei was also performed at the ARES facility [22], and it was also investigated at the $c\tau$ factory [23]. The Japan Hadron Facility (JHF) is essentially a kaon factory, thus it is producing large fluxes of hyperons that should allow a detailed study of hypernuclei. Furthermore, with a beam energy of 50 GeV, it will produce charmed and bottom hadrons with rather large intensity. So it is realistic to search for charmed and bottom hypernuclei at JHF. With the forthcoming facilities such as GSI-FAIR and J-PARC [24], it also would be possible to check whether the charmed hypernuclei exist or not. Recently, a measurement of the Λ_b^0 lifetime and mass in the decay channel $\Lambda_b^0 \to J/\psi(\mu^+\mu^-)\Lambda^0(p\pi^-)$ was reported in the ATLAS experiment [25].

Theoretically, this problem was revisited recently with the quark-meson coupling model and it was suggested that the heavy baryons containing a charm or a bottom quark will form charm or bottom hypernuclei [26]. The possibility of bound deuteron-like states, such as $N\Sigma_c$, $N\Xi_c'$, $N\Xi_{cc}$, $\Xi\Xi_{cc}$, and so on, were also investigated by several realistic phenomenological nucleon-nucleon interaction models [27,28]. However, it is inconclusive whether the two-body bound states in the $N\Lambda_c$ or $N\Lambda_b$ channel exist or not [16]. As $N\Lambda_c$ is the most fundamental charmed nucleon state, it is worthwhile to study it with various methods. Recently, the $N\Lambda_c$ system and relevant coupled channel effects were studied on the hadron level [29]. It is found that molecular bound states of $N\Lambda_c$ are plausible. Clearly the quark level study of the $N\Lambda_c$ system is interesting and necessary.

It is well known that the forces between nucleons (hadronic clusters of quarks) are qualitative, similar to the forces between atoms (molecular force). This molecular model of nuclear forces, the quark delocalization color screening model (QDCSM) [7], has been developed and extensively studied. In this model, quarks confined in one nucleon are allowed to delocalize to a nearby baryon and the confinement interaction between quarks in different baryon orbits is modified to include a color screening factor. The latter is a model description of the hidden color channel coupling effect [8]. The delocalization parameter is determined by the dynamics of the interacting quark system, this allows the quark system to choose the most favorable configuration through its own dynamics in a larger Hilbert space. The model gives a good description of NN and YN interactions and the properties of the deuteron [7].

It is also employed to calculate the baryon-baryon scattering phase shifts in the framework of the resonating group method (RGM), and the dibaryon candidates are also studied with this model [8,9].

In this work, we study the interactions of the $N\Lambda_c$ systems in QDCSM, in which the channel-coupling effects of $N\Sigma_c$ and $N\Sigma_c^*$ are considered. Our purpose is to understand the interaction properties of the $N\Lambda_c$ system and to see whether the $N\Lambda_c$ or $N\Sigma_c$ bound state, or a $N\Lambda_c - N\Sigma_c$ dynamically generated resonance can be formed. An extension of the study to the bottom case is also interesting, so we also investigate the $N\Lambda_b$ systems in the present work. The channel-coupling effects of $N\Sigma_b$ and $N\Sigma_b^*$ are also considered with this model.

The structure of this paper is as follows. After the Introduction, we present a brief introduction of the quark models used in Sec. II. Section III is devoted to the numerical results and discussions. The summary is shown in the last section.

II. THE QUARK DELOCALIZATION COLOR SCREENING MODEL (QDCSM)

The quark delocalization color screening model (QDCSM) used in the present work has been described in Refs. [7–9] in detail. Here, we just present the salient features of this model. The QDCSM Hamiltonian is

$$H = \sum_{i=1}^{6}\left(m_i + \frac{p_i^2}{2m_i}\right) - T_c + \sum_{i<j}[V^G(r_{ij}) + V^\chi(r_{ij}) + V^C(r_{ij})],$$

$$V^G(r_{ij}) = \frac{1}{4}\alpha_{s_{ij}}\lambda_i\cdot\lambda_j\left[\frac{1}{r_{ij}} - \frac{\pi}{2}\left(\frac{1}{m_i^2} + \frac{1}{m_j^2} + \frac{4\sigma_i\cdot\sigma_j}{3m_im_j}\right)\delta(r_{ij}) - \frac{3}{4m_im_jr_{ij}^3}S_{ij}\right],$$

$$V^\chi(r_{ij}) = \frac{1}{3}\alpha_{ch}\frac{\Lambda^2}{\Lambda^2 - m_\chi^2}m_\chi\left\{\left[Y(m_\chi r_{ij}) - \frac{\Lambda^3}{m_\chi^3}Y(\Lambda r_{ij})\right]\sigma_i\cdot\sigma_j + \left[H(m_\chi r_{ij}) - \frac{\Lambda^3}{m_\chi^3}H(\Lambda r_{ij})\right]S_{ij}\right\}\mathbf{F}_i\cdot\mathbf{F}_j, \quad \chi = \pi, K, \eta,$$

$$\qquad\qquad\qquad\qquad\qquad\qquad\qquad\qquad\qquad\qquad\qquad\qquad\qquad\qquad\qquad\qquad\qquad\qquad (1)$$

$$V^C(r_{ij}) = -a_c\lambda_i\cdot\lambda_j[f(r_{ij}) + V_0],$$

$$f(r_{ij}) = \begin{cases} r_{ij}^2 & \text{if } i, j \text{ occur in the same baryon orbit} \\ \frac{1-e^{-\mu r_{ij}^2}}{\mu} & \text{if } i, j \text{ occur in different baryon orbits,} \end{cases}$$

$$S_{ij} = \frac{(\sigma_i\cdot\mathbf{r}_{ij})(\sigma_j\cdot\mathbf{r}_{ij})}{r_{ij}^2} - \frac{1}{3}\sigma_i\cdot\sigma_j,$$

where S_{ij} is quark tensor operator, $Y(x)$, $H(x)$ and $G(x)$ are standard Yukawa functions [4], T_c is the kinetic energy of the center of mass, α_{ch} is the chiral coupling constant, determined as usual from the π-nucleon coupling constant. All other symbols have their usual meanings. Here, a phenomenological color screening confinement potential is used, and μ is the color screening parameter. For the NN system, it is determined by fitting the deuteron mass. In the present work, we take it as a common parameter for the $N\Lambda_c$, $N\Sigma_c$, and $N\Sigma_c^*$ channels, because no experimental data are available.

In this work, we take the parameters for the light-flavor quark system from our previous work [9], which give a satisfactory description for the energies of the octet and decuplet baryon ground states, the binding energy of the deuteron, the scattering phase shifts of NN and YN. The additional parameters needed in the present work are those associated with the charm and bottom quarks, the charm and

bottom quark masses m_c and m_b, the coupling constants α_s in the V^G for light and heavy quark pairs uc, sc, ub, and sb (which are labeled as $\alpha_{s_{uc}}$, $\alpha_{s_{sc}}$, $\alpha_{s_{ub}}$, and $\alpha_{s_{sb}}$ in Table I). They are fixed by an overall fitting to the masses of the charmed and bottom baryons. The values of those parameters are listed in Table I. The corresponding masses of the charmed and bottom baryons are shown in Table II.

The quark delocalization in QDCSM is realized by specifying the single particle orbital wave function of QDCSM as a linear combination of the left and right Gaussian, the single particle orbital wave functions used in the ordinary

TABLE II. The masses (in MeV) of the charmed and bottom baryons obtained from QDCSM. Experimental values are taken from the Particle Data Group (PDG) [30].

	Σ_c	Σ_c^*	Λ_c	Ξ_c^*	Ξ_c	$\Xi_c^{'}$	Ω_c	Ω_c^*
Expt.	2455	2520	2286	2645	2467	2575	2695	2770
QDCSM	2472	2487	2286	2590	2496	2576	2695	2708
	Σ_b	Σ_b^*	Λ_b	Ξ_b	Ω_b			
Expt.	5811	5832	5619	5791	6071			
QDCSM	5810	5817	5619	5848	6071			

TABLE I. Model parameters associated with the charm and bottom quarks.

m_c (MeV)	m_b (MeV)	$\alpha_{s_{uc}}$	$\alpha_{s_{sc}}$	$\alpha_{s_{ub}}$	$\alpha_{s_{sb}}$
1596	5000	0.396	0.576	0.553	0.605

TABLE III. The $N\Lambda_c$ and $N\Lambda_b$ states and the channels coupled to them.

	Channels
$J^P = 0^+$	$N\Lambda_c(^1S_0), N\Sigma_c(^1S_0), N\Sigma_c^*(^5D_0)$
$J^P = 1^+$	$N\Lambda_c(^3S_1), N\Sigma_c(^3S_1), N\Sigma_c^*(^3S_1),$
	$N\Lambda_c(^3D_1), N\Sigma_c(^3D_1), N\Sigma_c^*(^3D_1)$
	$N\Sigma_c^*(^5D_1)$
$J^P = 0^+$	$N\Lambda_b(^1S_0), N\Sigma_b(^1S_0), N\Sigma_b^*(^5D_0)$
$J^P = 1^+$	$N\Lambda_b(^3S_1), N\Sigma_b(^3S_1), N\Sigma_b^*(^3S_1),$
	$N\Lambda_b(^3D_1), N\Sigma_b(^3D_1), N\Sigma_b^*(^3D_1),$
	$N\Sigma_b^*(^5D_1)$

quark cluster model,

$$\psi_\alpha(\mathbf{S}_i, \epsilon) = (\phi_\alpha(\mathbf{S}_i) + \epsilon\phi_\alpha(-\mathbf{S}_i))/N(\epsilon),$$
$$\psi_\beta(-\mathbf{S}_i, \epsilon) = (\phi_\beta(-\mathbf{S}_i) + \epsilon\phi_\beta(\mathbf{S}_i))/N(\epsilon),$$
$$N(\epsilon) = \sqrt{1 + \epsilon^2 + 2\epsilon e^{-S_i^2/4b^2}}, \quad (2)$$
$$\phi_\alpha(\mathbf{S}_i) = \left(\frac{1}{\pi b^2}\right)^{3/4} e^{-\frac{1}{2b^2}(\mathbf{r}_\alpha - \mathbf{S}_i/2)^2},$$
$$\phi_\beta(-\mathbf{S}_i) = \left(\frac{1}{\pi b^2}\right)^{3/4} e^{-\frac{1}{2b^2}(\mathbf{r}_\beta + \mathbf{S}_i/2)^2}.$$

Here $\mathbf{S}_i$, $i = 1, 2, ..., n$ are the generating coordinates, which are introduced to expand the relative motion wave function [8]. The mixing parameter $\epsilon(\mathbf{S}_i)$ is not an adjusted one but determined variationally by the dynamics of the multiquark system itself. This assumption allows the multiquark system to choose its favorable configuration in the interacting process. It has been used to explain the crossover transition between hadron phase and quark-gluon plasma phase [31].

III. THE RESULTS AND DISCUSSIONS

Here we perform a dynamical investigation of the $N\Lambda_c$ system with $I = \frac{1}{2}$ and $J^P = 0^+$ or 1^+ in the QDCSM. The resonating group method (RGM), described in more detail in Ref. [32], is used here. The channel coupling effects are also considered. It is a three-channel problem for $J^P = 0^+$ and seven-channel problem for $J^P = 1^+$. The labels of channels are listed in Table III.
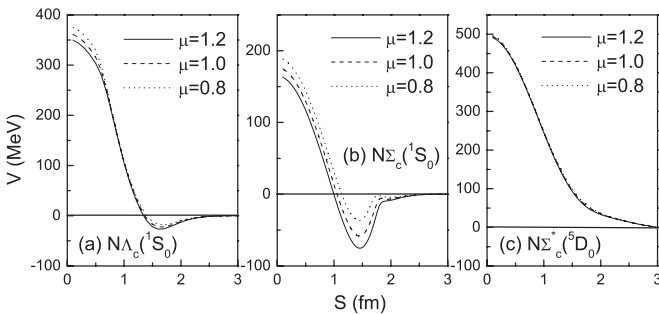

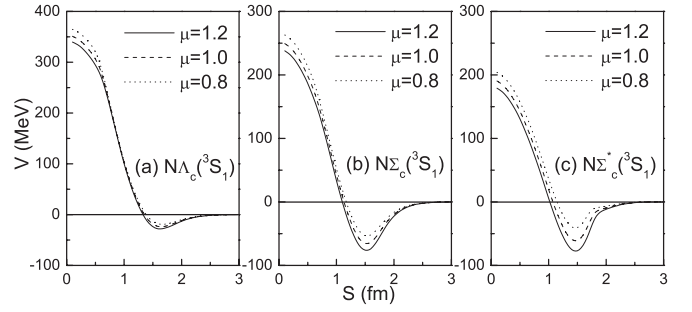FIG. 1. The potentials of different channels for the $J^P = 0^+$ case of the $N\Lambda_c$ system.

FIG. 2. The potentials of S-wave different channels for the $J^P = 1^+$ case of the $N\Lambda_c$ system.

First, the effective potentials between N and Λ_c (Σ_c) are calculated and shown in Figs. 1–3, because an attractive potential is necessary for forming a bound state or resonance. The effective potential between two colorless clusters is defined as $V(S) = E(S) - E(\infty)$, where $E(S)$ is the diagonal matrix element of the Hamiltonian of the system in the generating coordinate. As mentioned in Sec. II, a phenomenological color screening confinement potential is introduced in our model. For the multiquark systems with a heavy quark, because no experimental data are available, we take three different values of μ ($\mu = 1.2, 1.0, 0.8$), to test the dependence of our results on this parameter.

For the $J^P = 0^+$ case (Fig. 1), one sees that the potentials are both attractive for the $^1S_0$ channels $N\Lambda_c$ and $N\Sigma_c$. While for the channel $N\Sigma_c^*(^5D_0)$, the potential is repulsive and so no bound state can be formed in this case. The attraction between N and Σ_c is larger than the one between N and Λ_c. In Fig. 1, we also find that larger values of μ gives rise to deeper attractions for the attractive channels. However, for the repulsive $N\Sigma_c^*(^5D_0)$ channel, the potentials are quantitatively the same with three different values of μ.

For the $J^P = 1^+$ case (Fig. 2), we can see that the potentials are all attractive for the $^3S_1$ channels $N\Lambda_c$, $N\Sigma_c$, and $N\Sigma_c^*$. The attraction between N and Σ_c^* is a little smaller than that between N and Σ_c, but they are both larger than the one
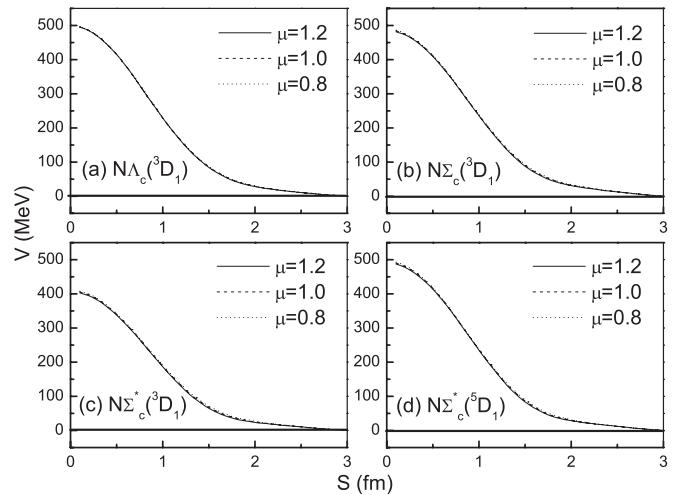

FIG. 3. The potentials of D-wave different channels for the $J^P = 1^+$ case of the $N\Lambda_c$ system.

TABLE IV. The binding energy of $N\Sigma_c$ and $N\Sigma_c^*$ (in MeV).

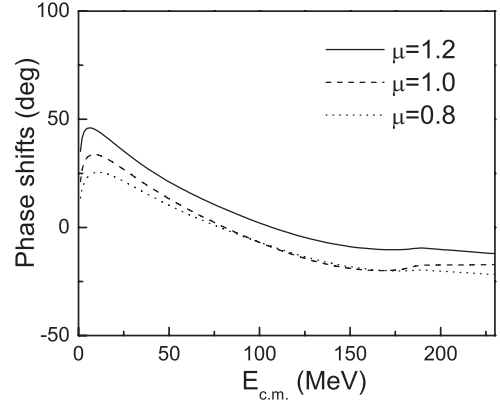|	$N\Sigma_c(^1S_0)$	$N\Sigma_c(^3S_1)$	$N\Sigma_c^*(^3S_1)$
$\mu = 1.2$	5.3	13.8	8.5
$\mu = 1.0$	ub	7.0	ub
$\mu = 0.8$	ub	1.0	ub

between N and Λ_c. While for all D-wave channels (see Fig. 3) they are all strongly repulsive, therefore no bound state will be found in D-wave channels. For the dependence of potentials on the different values of μ, the case is the same as that for the $J^P = 0^+$ system.

In order to see whether or not there is a $N\Lambda_c$ or $N\Sigma_c^*$ or $N\Sigma_c^*$ bound state, a dynamic calculation is needed. Here we solved the RGM equation for a bound-state problem. Expanding the relative motion wave function between two clusters in the RGM equation by Gaussians, the integrodifferential equation of RGM can be reduced to an algebraic equation, the generalized eigenequation. The energy of the system can be obtained by solving the eigenequation. In the calculation, the baryon-baryon separation is taken to be less than 6 fm (to keep the matrix dimension manageably small). The single channel calculation shows that the energy of $N\Lambda_c$ is above its threshold, the sum of the masses of N and Λ_c. It is reasonable, because the attraction between N and Λ_c is too weak to tie the two particles together. At the same time, due to the stronger attraction, the energies of $N\Sigma_c$ and $N\Sigma_c^*$ are below their corresponding thresholds. The binding energy of $N\Sigma_c$ and $N\Sigma_c^*$ states are listed in Table IV, in which 'ub' means unbound. From the table, one sees that $N\Sigma_c(^3S_1)$ is always bound, the binding energy is around $1 \sim 13.8$ MeV with three different values of μ. For $N\Sigma_c(^1S_0)$ and $N\Sigma_c^*(^3S_1)$ states, they are bound only for the case with large μ ($\mu = 1.2$). When the value of μ decreases, they become unbound.

Because state $N\Sigma_c$ or $N\Sigma_c^*$ can be coupled to state $N\Lambda_c$, and the channel coupling will shift the energy of the state, a channel coupling calculation is needed to check whether the state $N\Sigma_c$ or $N\Sigma_c^*$ can survive with respect to the channel-coupling effect. In the nonstrange dibaryon search, the single channel calculations give several bound states, $IJ = 01, 10, 03, \ldots \Delta\Delta$ states. However, when these states couple to corresponding NN states, only the $IJ = 03\Delta\Delta$ state appears as a resonance in the NN scattering phase shifts, other states disappeared due to the channel coupling effect of the NN state [8]. The similar results are obtained for dibaryon resonances with strangeness [9]. By analogy, one may expect either a $N\Sigma_c$ or $N\Sigma_c^*$ resonance in the $N\Lambda_c$ scattering process or the resonance state will disappear if it is pushed above the $N\Sigma_c$ or $N\Sigma_c^*$ threshold by coupling to the $N\Lambda_c$ channel. In

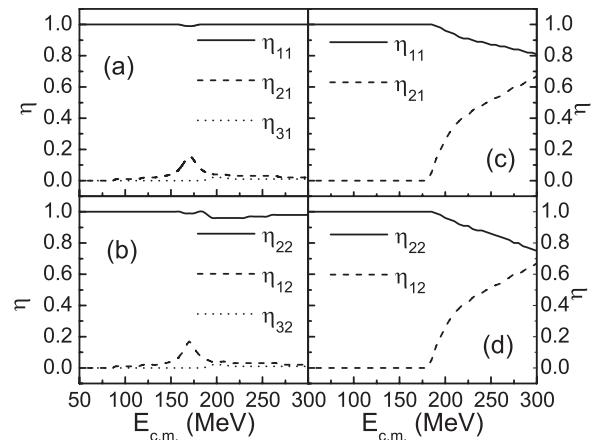TABLE V. $N\Sigma_c$, $N\Sigma_c^*$, or resonance mass in MeV.

	$\mu = 1.2$		$\mu = 1.0$		$\mu = 0.8$	
	$cc1/cc2$	$cc3$	$cc1/cc2$	$cc3$	$cc1/cc2$	$cc3$
$N\Sigma_c(^3S_1)$	3394	3389	3402	3397	3408	3404
$N\Sigma_c^*(^3S_1)$	3415	nr	3425	nr	nr	nr

FIG. 4. $N\Lambda_c(^1S_0)$ phase shifts with two channels [$N\Sigma_c(^1S_0)$ and $N\Sigma_c^*(^5D_0)$] coupling.

addition, we also want to know whether the bound state of $N\Lambda_c$ can be formed or not with the channels coupling. The results are shown in Table V and Fig. 4. There are several features which are discussed below.

First, there is no any $N\Lambda_c$ bound state formed in the present channel-coupling calculation, which is different from the conclusion on the hadron level [29]. Taking the $J^P = 0^+$ state as an example, we perform a three-channel coupling calculation, $N\Lambda_c(^1S_0)$, $N\Sigma_c(^1S_0)$, and $N\Sigma_c^*(^5D_0)$. Although the coupling between the $N\Lambda_c(^1S_0)$ and $N\Sigma_c(^1S_0)$ channels is through the central force, it is not strong enough to form a $N\Lambda_c(^1S_0)$ bound state, which is consistent with the calculation on the hadron level [29]. The effect of the $N\Sigma_c^*(^5D_0)$ channel coupling to $N\Lambda_c(^1S_0)$ is very small, because there only the tensor force plays a role in our quark model calculation. While in Ref. [29] on the hadron level, the tensor force is important and the bound state of $N\Lambda_c(^1S_0)$ is plausible by the channel coupling of $N\Sigma_c^*(^5D_0)$.

Secondly, the channel coupling calculation of $N\Lambda_c(^1S_0)$ scattering phase shifts (see Fig. 4) does not show any resonance, even if the $N\Sigma_c(^1S_0)$ is a bound state with binding energy 5.3 MeV ($\mu = 1.2$) in the single-channel calculation. The disappearance of the resonance is due to the channel

FIG. 5. The transmission and reflection coefficients. (a), (b) $N\Lambda_c(^3S_1)$-$N\Lambda_c(^3D_1)$-$N\Sigma_c(^3S_1)$), (c), (d) $N\Lambda_c(^1S_0)$-$N\Sigma_c(^1S_0)$).
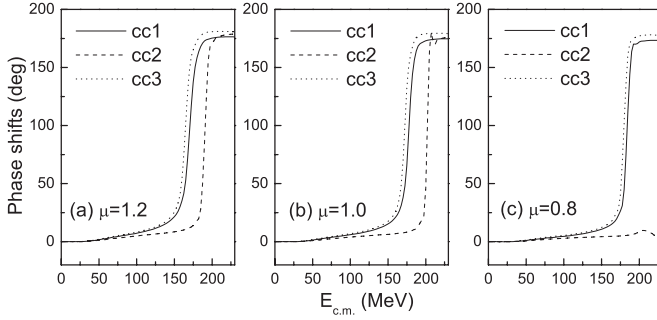
FIG. 6. $N\Lambda_c(^3D_1)$ phase shifts with different numbers of coupled channels, as described in more detail in the text.

coupling to the $N\Lambda_c$ channel pushing the energy of $N\Sigma_c$ above its threshold. To show the coupling strength of these two channels, the transmission and reflection coefficients [33] of these two channels are shown in Fig. 5. In Fig. 4, we also find that larger values of μ makes deeper attractions in this channel.

Thirdly, there are resonance states of $N\Sigma_c(^3S_1)$ and $N\Sigma_c^*(^3S_1)$ that appear in the $N\Lambda_c(^3D_1)$ scattering process. The masses of the resonances are shown in Table V, where 'nr' means no resonance; $cc1$ and $cc2$ denote two-channel coupling, $N\Lambda_c(^3D_1)$-$N\Sigma_c(^3S_1)$ and $N\Lambda_c(^3D_1)$-$N\Sigma_c^*(^3S_1)$; $cc3$ means channel coupling with seven channels, which are listed in Table III. From Table V, we can see that by coupling to open channel $N\Lambda_c(^3D_1)$, the energies of bound states are pushed down a little, which means that the mass shifts of the bound state are dominated by the open D-wave scattering states above the energy of the stand-alone bound state. The results are consistent with those of $N\Lambda$ scattering [9]. Comparing the results of $cc1$ and $cc3$, we found that the $N\Lambda_c(^3S_1)$ channel has a very small effect on the coupling of $N\Lambda_c(^3D_1)$-$N\Sigma_c(^3S_1)$. The related transmission and reflection coefficients are also shown in Fig. 5. From Fig. 5, we can see that the coupling between $N\Lambda_c(^3S_1)$ and $N\Sigma_c(^3S_1)$ is very weak compared to the $J = 0$ case. Taking the case of $\mu = 1.2$ as an example: for the case of $cc1$, the $N\Sigma_c(^3S_1)$ state decays to state $N\Lambda_c(^3D_1)$ only through tensor interaction, and the energy of the state $N\Sigma_c(^3S_1)$ is pushed down a little ~ 3 MeV; for the case of $cc2$, the $N\Sigma_c^*(^3S_1)$ state decays to state $N\Lambda_c(^3D_1)$ also through tensor interaction, and the mass shift of the energy of the state $N\Sigma_c^*(^3S_1)$ is ~ 2 MeV; for the case of $cc3$, the S-wave states $N\Sigma_c(^3S_1)$ and $N\Sigma_c^*(^3S_1)$ are coupled by central interactions, so the channel coupling effect is a little larger, pushing the energy of $N\Sigma_c^*(^3S_1)$ above its threshold. In the scattering phase shifts of $N\Lambda_c(^3D_1)$, the resonance energy of $N\Sigma_c(^3S_1)$ is ~ 8 MeV lower than its binding energy in the stand-alone calculation, while the resonance $N\Sigma_c^*(^3S_1)$

TABLE VI. The binding energy of $N\Sigma_b$ and $N\Sigma_b^*$ (in MeV).

	$N\Sigma_b(^1S_0)$	$N\Sigma_b(^3S_1)$	$N\Sigma_b^*(^3S_1)$
$\mu = 1.2$	1.2	9.5	ub
$\mu = 1.0$	ub	3.7	ub
$\mu = 0.8$	ub	ub	ub

TABLE VII. $N\Sigma_b$, $N\Sigma_b^*$, or resonance mass in MeV.

	$\mu = 1.2$		$\mu = 1.0$		$\mu = 0.8$	
	$cc1/cc2$	$cc3$	$cc1/cc2$	$cc3$	$cc1/cc2$	$cc3$
$N\Sigma_b(^3S_1)$	6735	6733	6745	6740	6748	6743
$N\Sigma_b^*(^3S_1)$	6755	nr	nr	nr	nr	nr

disappears. All these resonances can be seen in the $N\Lambda_c(^3D_1)$ scattering phase shifts, which are shown in Fig. 6. The results of $\mu = 1.0$ and $\mu = 0.8$ are qualitatively similar to that of $\mu = 1.2$, but with a little higher resonance mass. Here, we also notice that for the $N\Sigma_c^*(^3S_1)$ channel with $\mu = 1.0$, it is unbound in the single channel calculation (see Table IV). However, it becomes a resonance state with a mass of 3425 MeV (see in Table V) by coupling to the open $N\Lambda_c(^3D_1)$ channel. From the results, we find the state $N\Sigma_c(^3S_1)$ is a good resonance candidate with energies of 3389–3404 MeV in our calculation. However, the resonance can only be seen in the $N\Lambda_c(^3D_1)$ channel. The direct channel coupling effect between the $N\Lambda_c(^3S_1)$ and $N\Sigma_c(^3S_1)$ channels by the central force is so weak that no resonance appears in the $N\Lambda_c(^3S_1)$ scattering phase shift.

In the previous discussion, the $N\Lambda_c$ system was investigated and the resonance state was found. Because of the heavy flavor symmetry, we also extend the study to the bottom case of the $N\Lambda_b$ system. The numerical results for the $N\Lambda_b$ system are listed in Tables VI and VII and Figs. 7 and 8. The results are similar to the $N\Lambda_c$ system. From Table VII and Fig. 8, we also find the state $N\Sigma_b(^3S_1)$ is a good resonance candidate with energies of 6733–6743 MeV in our quark model.

IV. SUMMARY

In this work, we perform a dynamical calculation of the $N\Lambda_c$ system with $I = \frac{1}{2}$ and $J^P = 0^+$ or 1^+ by solving the RGM equation in the framework of QDCSM. Our results show that the interaction between N and Λ_c is attractive, but it is not strong enough to form $N\Lambda_c$ bound states. The channel coupling does not help much, the state $N\Lambda_c(^1S_0)$ is still not bound, although the coupling of the $N\Lambda_c(^1S_0)$ and $N\Sigma_c(^1S_0)$
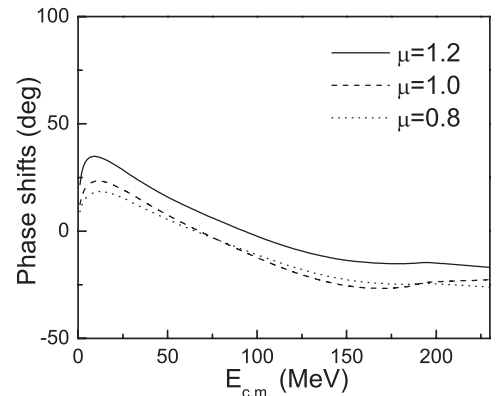

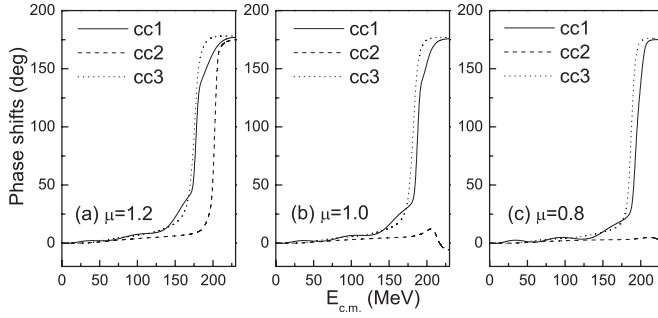FIG. 7. $N\Lambda_b(^1S_0)$ phase shifts with two channels [$N\Sigma_b(^1S_0)$ and $N\Sigma_b^*(^5D_0)$] coupling.

FIG. 8. $N\Lambda_b(^3D_1)$ phase shifts with different numbers of coupled channels, as described in more detail in the text.

channels is through the central interaction. This result is consistent with the result of the calculation on the hadron level [29]. However, the effect of the $N\Sigma_c^*(^5D_0)$ channel coupling, which depends on the tensor force, is small in our calculation, while in the calculation on the hadron level [29], the tensor force is shown to be important and the bound state of $N\Lambda_c(^1S_0)$ is formed by the channel coupling of $N\Sigma_c^*(^5D_0)$. Further investigation should be done to understand the difference between the approaches on the hadron level and the quark level. It will help us to understand the hadron-hadron interaction and exotic quark states, which is one of the important topics in the temporary hadron physics.

In the present work, we find that the attraction between N and Σ_c is strong enough to form a bound state $N\Sigma_c(^3S_1)$, it becomes a resonance state with the resonance mass of 3389–3404 MeV when coupling to the open $N\Lambda_c$ D-wave channel. The $N\Lambda_c$ scattering process is studied in our model, and the $N\Sigma_c(^3S_1)$ resonance state can be seen in the $N\Lambda_c(^3D_1)$ scattering phase shifts. An extension of the study to the bottom case has also been done. The results of the $N\Lambda_b$ system is similar to the $N\Lambda_c$ system, and there exists a $N\Sigma_b(^3S_1)$ resonance state with an energy of 6733–6743 MeV in our quark model.

In the present calculation, only the systems with $I = \frac{1}{2}$ and $J^P = 0^+$ or 1^+ are studied. The other two-body systems, $N\Xi_c$, $\Lambda\Lambda_c$, $\Sigma\Sigma_c$, $\Lambda\Sigma_c$, and so on, with different angular momenta would have similar properties, they should be investigated in various models on the hadron level and quark level as well.

[1] R. Machleidt, Adv. Nucl. Phys. **19**, 189 (1989), and references therein.

[2] Th. A. Rijken, Phys. Rev. C **73**, 044007 (2006); Th. A. Rijken and Y. Yamamoto, *ibid.* **73**, 044008 (2006).

[3] E. Epelbaum, H. W. Hammer, and Ulf-G. Meissner, Rev. Mod. Phys. **81**, 1773 (2009), and reference therein.

[4] A. Valcarce, H. Garcilazo, F. Fernandez, and P. Gonzalez, Rep. Prog. Phys. **68**, 965 (2005), and reference therein.

[5] Y. Fujiwara, C. Nakamoto, and Y. Suzuki, Phys. Rev. Lett. **76**, 2242 (1996).

[6] Z. Y. Zhang, Y. W. Yu, P. N. Shen *et al.*, Nucl. Phys. A **625**, 59 (1997); L. R. Dai, Z. Y. Zhang, Y. W. Yu, and P. Wang, *ibid.* **727**, 321 (2003).

[7] F. Wang, G. H. Wu, L. J. Teng, and T. Goldman, Phys. Rev. Lett. **69**, 2901 (1992); G. H. Wu, L. J. Teng, J. L. Ping, F. Wang, and T. Goldman, Phys. Rev. C **53**, 1161 (1996); G. H. Wu, J. L. Ping, L. J. Teng *et al.*, Nucl. Phys. A **673**, 279 (2000); J. L. Ping, F. Wang, and T. Goldman, *ibid.* **657**, 95 (1999); H. R. Pang, J. L. Ping, F. Wang, and T. Goldman, Phys. Rev. C **65**, 014003 (2001).

[8] J. L. Ping, F. Wang, and T. Goldman, Nucl. Phys. A **688**, 871 (2001); J. L. Ping, H. R. Pang, F. Wang, and T. Goldman, Phys. Rev. C **65**, 044003 (2002); L. Z. Chen, H. R. Pang, H. X. Huang, J. L. Ping, and F. Wang, *ibid.* **76**, 014001 (2007); J. L. Ping, H. X. Huang, H. R. Pang, F. Wang, and C. W. Wong, *ibid.* **79**, 024001 (2009); H. X. Huang, P. Xu, J. L. Ping, and F. Wang, *ibid.* **84**, 064001 (2011).

[9] M. Chen, H. X. Huang, J. L. Ping, and F. Wang, Phys. Rev. C **83**, 015202 (2011).

[10] J. J. Wu, R. Molina, E. Oset, and B. S. Zou, Phys. Rev. Lett. **105**, 232001 (2010); Phys. Rev. C **84**, 015202 (2011).

[11] W. L. Wang, F. Huang, Z. Y. Zhang, and B. S. Zou, Phys. Rev. C **84**, 015203 (2011).

[12] V. Shklyar, G. Penner, and U. Mosel, Eur. Phys. J. A **21**, 445 (2004); A. Usov and O. Scholten, Phys. Rev. C **72**, 025205 (2005); A. V. Sarantsev, V. A. Nikonov, A. V. Anisovich, E. Klempt, and U. Thoma, Eur. Phys. J. A **25**, 441 (2005).

[13] O. Krehl, C. Hanhart, C. Krewald, and J. Speth, Phys. Rev. C **62**, 025207 (2000).

[14] N. Isgur and G. Karl, Phys. Rev. D **18**, 4187 (1978); S. Capstick and N. Isgur, *ibid.* **34**, 2809 (1986).

[15] F. Huang, W. L. Wang, Z. Y. Zhang, and Y. W. Yu, Phys. Rev. C **76**, 018201 (2007).

[16] C. B. Dover and S. H. Kahana, Phys. Rev. Lett. **39**, 1506 (1977).

[17] A. A. Tyapkin, Sov. J. Nucl. Phys. **22**, 89 (1976).

[18] G. Bhamathi, Phys. Rev. C **24**, 1816 (1981).

[19] H. Bando and M. Bando, Phys. Lett. B **109**, 164 (1982); H. Bando and S. Nagata, Prog. Theor. Phys. **69**, 557 (1983); H. Bando, Prog. Theor. Phys. Suppl. **81**, 197 (1985).

[20] B. F. Gibson, C. B. Dover, G. Bhamathi, and D. R. Lehman, Phys. Rev. C **27**, 2805 (1983).

[21] Y. A. Batusov *et al.*, JETP Lett. **33**, 52 (1981).

[22] T. Bressani and F. Iazzi, Nuovo Cimento A **102**, 597 (1989).

[23] S. A. Buyatov, V. V. Lyukov, N. I. Strakov, and V. A. Tsarev, Nuovo Cimento A **104**, 1361 (1991).

[24] J. Riedl, A. Schafer, and M. Stratmann, Eur. Phys. J. C **52**, 987 (2007).

[25] ATLAS Collaboration, arXiv:1207.2284v1.

[26] K. Tsushima and F. C. Khanna, Phys. Lett. B **552**, 138 (2003); Phys. Rev. C **67**, 015211 (2003).

[27] F. Fromel, B. Julia-Diaz, and D. O. Riska, Nucl. Phys. A **750**, 337 (2005).

[28] B. Julia-Diaz and D. O. Riska, Nucl. Phys. A **755**, 431 (2005).

[29] Y. R. Liu and M. Oka, Phys. Rev. D **85**, 014015 (2012).

[30] J. Beringer *et al.* (Particle Data Group), Phys. Rev. D **86**, 010001 (2012).

[31] M. M. Xu, M. L. Yu, and L. S. Liu, Phys. Rev. Lett. **100**, 092301 (2008).

[32] M. Kamimura, Suppl. Prog. Theor. Phys. **62**, 236 (1977).

[33] Y. Fujiwara, C. Nakamoto, and Y. Suzuki, Prog. Theor. Phys. **94**, 353 (1994).